Dalton Transactions

RSC Publishing

PAPER

View Article Online
View Journal | View Issue

Cite this: *Dalton Trans.*, 2013, **42**, 2530

Single-site N–N bond cleavage by Mo(IV): possible mechanisms of hydrazido(1–) to nitrido conversion†

Stephen A. DiFranco, Richard J. Staples and Aaron L. Odom*

Received 5th November 2012,
Accepted 20th November 2012

DOI: 10.1039/c2dt32643d

www.rsc.org/dalton

$Mo(NMe_2)_4$ and the tridentate, dipyrrolyl ligand H_2dpma^{mes} were found to form 5-coordinate $Mo(NMe_2)_2(dpma^{mes})$ (**1**), which exhibits spin-crossover behaviour in solution. The complex is a ground state singlet with a barrier of 1150 cm^{-1} for production of the triplet in d_8-toluene. The complex reacts with 1,1-disubstituted hydrazines or *O*-benzylhydroxylamine to produce nitrido $MoN(NMe_2)(dpma^{mes})$. The mechanism of the 1,1-dimethylhydrazine reaction with **1** was examined along with the mechanism of substitution of NMe_2 with H_2NNMe_2 in a diamagnetic zirconium analogue. The proposed mechanism involves production of a hydrazido(1–) intermediate, $Mo(NMe_2)(NHNMe_2)(dpma^{mes})$, which undergoes an α,β-proton shift and N–N bond cleavage with metal oxidation to form the nitrido. The rate law for the reaction was found to be $-d[\mathbf{1}]/dt = k_{obs}[\mathbf{1}][hydrazine]$ by initial rate experiments and examination of the full reaction profile. This conversion from hydrazido(1–) to nitrido is somewhat analogous to the proposed mechanism for O–O bond cleavage in some peroxidases.

Introduction

The reduction of dinitrogen is arguably one of the most important reactions ever discovered[1] and is the starting point for the production of the majority of nitrogen-containing compounds with applications from fertilizers to pharmaceuticals. In accordance with the importance of the reaction, numerous studies have been carried out on the biological systems responsible (nitrogenases),[2] the industrial process[3] for production of ammonia (Haber–Bosch), and other systems capable of nitrogen reduction.[1]

The naturally occurring systems can, but do not always, contain molybdenum in the active site of the cofactor but do include an iron–sulfur cluster.[4]

The mechanism of the N–N cleavage has been divided into two general forms depending largely on the sites of protonation, which have been dubbed the Distal and Alternating Mechanisms. In Scheme 1 are some of the steps commonly attributed to these cycles.[5]

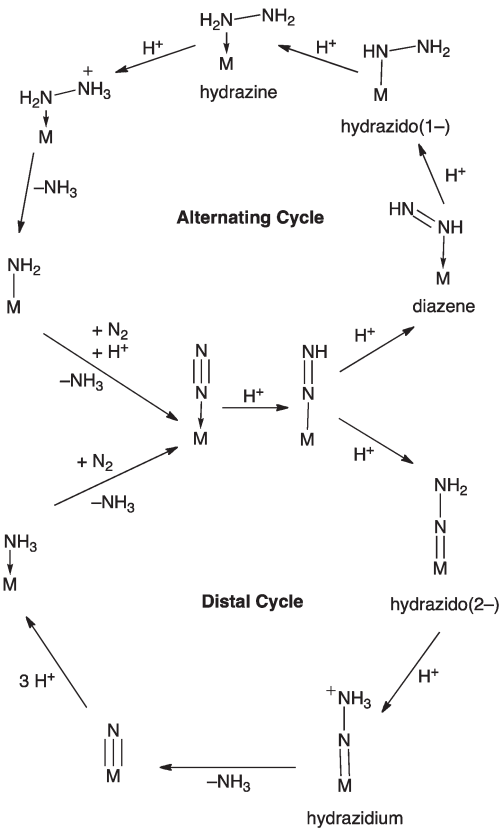

Scheme 1 Two catalytic cycles often discussed for N–N bond cleavage. The exact steps for electron transfer are left ambiguous.

Michigan State University, Department of Chemistry, 578 S. Shaw Ln, East Lansing, MI 48824, USA. E-mail: odom@chemistry.msu.edu

†Electronic supplementary information (ESI) available: Determination of rate constants in Table 1, initial rate experiments on H_2NNMe_2 with **1**, initial rate experiments on concentration of **1**, details for thermal conversion of *syn*-**2** and *anti*-**2**, UV-Vis trace of *anti*-**2** formation using H_2NNMe_2 with **1**, X-ray powder diffraction on samples of **1**, Eyring Plot for H_2NNMe_2 with **1**, additional mechanistic discussions, kinetics on the reaction of H_2NNMe_2 with **3**, and details for the single crystal X-ray diffraction experiment. CCDC 909421–909426. For ESI and crystallographic data in CIF or other electronic format see DOI: 10.1039/c2dt32643d

Frequently in molybdenum- and tungsten-based systems, the cleavage of the nitrogen–nitrogen single bond required in these reactions is proposed to occur through a hydrazido(2–)[6] intermediate that becomes protonated to an ammonium imido (hydrazidium) complex (Distal Cycle of Scheme 1). If the metal center has the two electrons required for N–N bond cleavage, this can occur through simple N–N bond scission in Mo(IV) and W(IV) hydrazidium intermediates.

Conversely, some molecular iron-based systems for nitrogen reduction often have been suggested to proceed through diazene intermediates (Alternating Cycle of Scheme 1).[7]

In this report, we demonstrate facile single-site cleavage of an N–N bond through production of a Mo(IV) hydrazido(1–). The available data suggest that molybdenum systems can proceed from hydrazido(1–) to nitrido by way of α,β-proton migration. Consequently, pathways that include complexed diazene,[8] hydrazido(1–), and nitrido may be viable for Mo-based N–N bond cleavage.

Results and discussion

Synthesis and characterization of compounds

The ancillary ligand chosen was a sterically more substantial version of the pyrrole-based *N*,*N*-di(pyrrolyl-α-methyl)-*N*-methylamine, dpma, which we have employed in several catalytic and stoichiometric studies previously.[9] For this chemistry, mesityl groups were installed[10] into the remaining α-positions of the pyrroles. The synthesis of the new ligand, H_2dpma^{mes}, is shown in Fig. 1 along with the synthesis and structure of the molybdenum dimethylamido derivative prepared by transamination on $Mo(NMe_2)_4$.[11]

The structure of 5-coordinate **1** is very nearly halfway between trigonal bipyramidal (tbp) and square pyramidal (sp). The largest angle subtended at molybdenum is 164.9(1)° (α) for N3–Mo1–N5 and the second largest is 129.1(1)° (β) for N1–Mo1–N2. The value for τ from $\tau = (\alpha - \beta)/60 = 0.60$, where a value of 1 is for tbp and a value of 0 is for sp.[12]

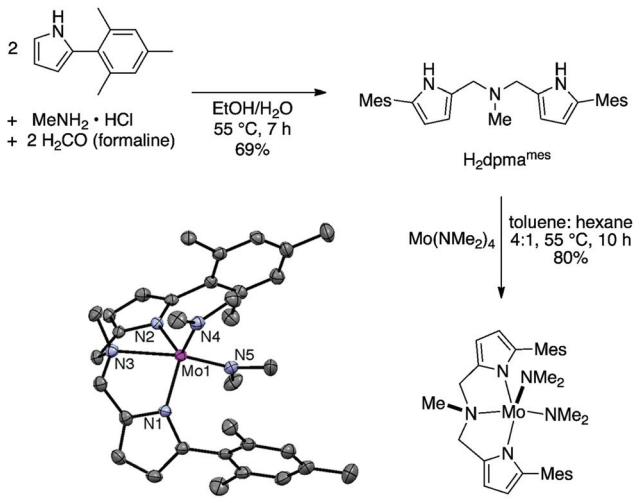

Fig. 1 Synthesis and structure of $Mo(NMe_2)_2(dpma^{mes})$ (**1**). Hydrogens and a toluene solvent molecule found in the lattice are omitted from the structure.

Due to weaker donation of the pyrroles to the Mo center relative to the dimethylamidos,[13] metal–N(pyrrole) distances are usually significantly longer than metal–NMe_2 distances, and that is the case here. The average Mo–N(pyrrole) distance in the structure was determined to be 2.091(2) Å. The average Mo–NMe_2 distance was 1.917(2) Å. The much weaker donor nitrogen of the $dpma^{mes}$ had an Mo(1)–N(3) distance of 2.401(2) Å.

Magnetic susceptibility measurements in solution (Evan's method at 29.7 °C in d_8-toluene)[14] provided a μ_{eff} = 1.18 μ_B, well below the spin-only moment for high-spin d^2 of 2.87 μ_B and well below the value for the high spin *tert*-butylisonitrile adduct of the same compound **1**·$CNBu^t$ (*vide infra*). SQUID magnetometry on **1** in the solid state suggests the compound is a ground-state singlet. Even at room temperature, the compound exhibited no detectable paramagnetism as a solid. This suggests that the compound has a thermally accessible triplet state in solution but not in the solid state, likely because an isomerization is required to access the higher spin state.

Examination of the magnetism in solution was done over the accessible temperature range (~230–350 K), bound on the lower end by the solubility of the compound and on the higher end by its stability in solution. The data were fit using the expression of Gütlich and coworkers (eqn (1)).[15] In our case, none of the resonances in the ^{1}H NMR could be followed over the entire temperature range due to broadening. Consequently, we used an internal standard of $PhSiMe_3$ in the solution with a capillary containing d_8-toluene and reference $PhSiMe_3$ to follow the contact shift due to the paramagnetic species.

$$\delta = \frac{C}{T(1 + e^{\Delta G_{SC}/RT})} + \delta' \quad (1)$$

The value δ is the difference in ppm between the chemical shift of the methyl groups in the $PhSiMe_3$ reference (inside the capillary) and $PhSiMe_3$ in solution with **1**. In eqn (1), C is a constant, T is the temperature in Kelvin, and R is the gas constant.

Fitting the data to this equation gives the plot shown in Fig. 2. From the fit, ΔG_{SC}, the free energy associated with the spin crossover, was found to be 3.3 kcal mol^{-1} (1150 cm^{-1}). This is similar to values reported by Rothwell and coworkers for a large series of W(IV) complexes that exhibited spin crossover in solution.[16] For these cyclometallated 2,6-diphenylphenol compounds, $W(OC_6H_3Ph–C_6H_4–)_2L_2$, the energy difference varied from 358–1205 cm^{-1}, where L was a variety of different pyridine derivatives. Similarly, Schrock and co-workers have reported singlet–triplet spin crossover for the Mo(IV) species $[(Me_3SiNCH_2CH_2)_3N]MoNMe_2$.[17] The ΔG_{SC} value reported for this related system was ~1800 cm^{-1} based on reported enthalpy and entropy values.

Interestingly, there are now three different magnetic behaviours for reported Mo(IV) bis(dimethylamido) complexes bearing derivatives of the dpma ligand. In our paper using the

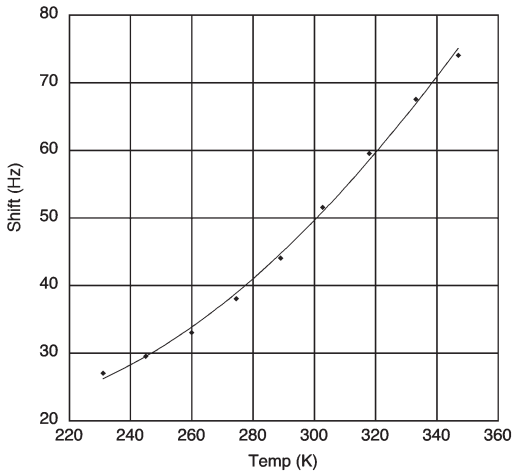

Fig. 2 Fit of the Me_3SiPh methyl group chemical shifts to eqn (1). The values for the fit parameters are $C = (2.31 \pm 0.61) \times 10^6$, $\Delta G = 3278 \pm 202$ cal mol^{-1}, and $\delta' = 18.3 \pm 2.0$ Hz.

less substituted pyrrolyl-based ligand,[18] 6-coordinate $Mo(NMe_2)_2(HNMe_2)$(dpma) was reported as a paramagnetic complex with a magnetic moment close to the spin-only value for two unpaired electrons. For this study, we confirmed that measurement on a freshly prepared sample; the value for this Mo(IV) 6-coordinate compound was found to be 2.48–2.40 μ_B from 210–300 K. Schrock and coworkers recently reported a related 5-coordinate compound $Mo(NMe_2)_2(tpa^{Ar})$, where tpa^{Ar} = tris[2-(3,5-trifluoromethylphenyl)pyrrolylmethyl)amine.[19] In this compound, which is structurally similar to **1**, two pyrrolyl substituents are bound to the metal center and the third is a "dangling" NH-pyrrole group. Interestingly, this compound is reported to have a mixture of broad and sharp lines in the NMR that were "slightly paramagnetically shifted". Consequently, this complex, contrary to **1**, seems to have a preponderance of the singlet complex in solution. In this report, **1** is a spin-crossover compound in solution and apparently diamagnetic in the solid state.

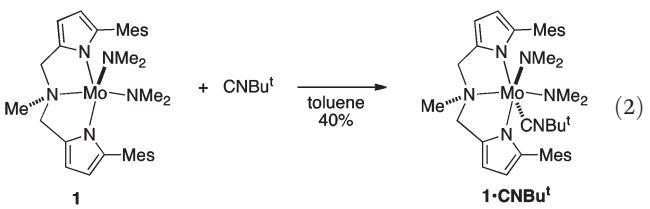

(2)

To examine the relationship between the electronic structure of **1** and its coordination number further, we prepared (eqn (2)) the *tert*-butylisonitrile adduct $Mo(NMe_2)_2(CNBu^t)$(dpma^{mes}) (**1**·$CNBu^t$). This adduct is quite similar structurally to **1** with the $CNBu^t$ ligand *trans* to one of the dimethylamido ligands and with the donor amine of the dpma^{mes} *trans* to the other NMe_2 group. The complex is high spin with $\mu_{eff} = 2.47$ μ_B like the previously reported 6-coordinate $Mo(NHMe_2)(NMe_2)_2$(dpma). The isonitrile adduct of **1** was also structurally characterized (see the ESI† for details).

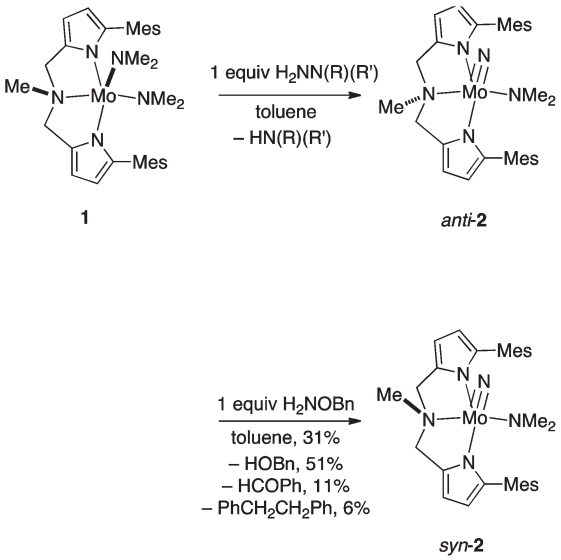

Scheme 2 Synthesis of *anti*-**2** and *syn*-**2** by N–N or N–O bond cleavage with isolated yields for the complexes. See Table 1 for hydrazines and yields of *anti*-**2**. Yields of by-products in the *O*-benzylhydroxylamine reaction are by GC-FID.

All of the 6-coordinate Mo(IV) dpma compounds observed thus far have had high spin ground states. The 5-coordinate Mo(IV) dpma complexes so far reported apparently have been spin crossover compounds with singlet ground states.

In an attempt to prepare the Mo(IV) terminal hydrazido(2–) complex, dimethylhydrazine was added to **1**. A diamagnetic product was obtained, the nitrido complex *anti*-Mo(N)(NMe_2)(dpma^{mes}) (*anti*-**2**) shown in Scheme 2.[20] The product has the nitrido nitrogen and methyl of the dpma^{mes} ligand on opposite sides of the plane defined by the Mo–N1(pyrrolyl)–N2(pyrrolyl) atoms. The yield of *anti*-**2** in this reaction by ^{1}H NMR was 75%, and the isolated yield was 74% (Table 1).

The structure of *anti*-**2** is shown in Fig. 3 (top). The structure of the Mo(VI) nitrido is best approximated as square pyramidal ($\tau = 0.02$).

The expectation in proceeding from the formally Mo(IV) complex **1** to the Mo(VI) complex **2** is that the bond distances should shorten. However, the Mo1–N(pyrrolyl) average distance in **2** is 2.127(3) Å, slightly longer than the 2.091(2) Å found in **1**. This lengthening of the pyrrolyl distance in **2** *vs.* **1** may be due to the rigidity of the dpma^{mes} ligand in this square planar derivative and the widening of the N(pyrrolyl)–Mo–N(pyrrolyl) angle from 129.06(7)° in **1** to 145.0(1)° in *anti*-**2**. The Mo1–N3(donor amine) distance in higher valent **2** was found to be 2.274(3) Å, whereas in **1** it was a much longer 2.401(2) Å. The Mo1–NMe_2 distance in **2** is 1.906(3) Å, which is not statistically different from the 1.917(2) Å average distance in **1**. The Mo–N(nitrido) distance in **2** was found to be 1.647(3) Å.

Other 1,1-disubstituted hydrazines react with **1** to give the same product (Scheme 2 and Table 1).

Addition of *O*-benzylhydroxylamine (Scheme 2) led to formation of the *syn*-isomer of **2**, where the amine donor methyl of the dpma^{mes} and nitrido nitrogen are on the same side of the Mo–N1(pyrrolyl)–N2(pyrrolyl) plane. The isomer *syn*-**2** was

Table 1 Rates and yields of the reactions of various substrates with **1** to form **2**

Substrate (H_2NX)	% Yield of **2**[a] (^{1}H NMR)	By-product % yield HX (GC-FID)	k_{obs}[c] ($M^{-1}s^{-1}$ 10^{-3})
H_2NNMe_2	75	—[b]	873 ± 5
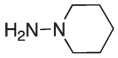	18	31	684 ± 2
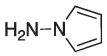	81	—[b]	146.8 ± 0.1
$H_2NN(Ph)Me$	82	91	135.8 ± 0.2
H_2NNPh_2	76	98	21.1 ± 0.1
H_2NOBn	31	51[e]	—[d]

[a] The product is **2**-*anti* except for the reaction with H_2NOBn which gave **2**-*syn*. [b] By-product yield was not determined. [c] Errors are from the fits and then propagated through the equations. [d] Reaction was too fast to measure using the methods employed here. [e] Yield given is for benzyl alcohol, but 3 by-products were identified. See the Experimental and Scheme 2.

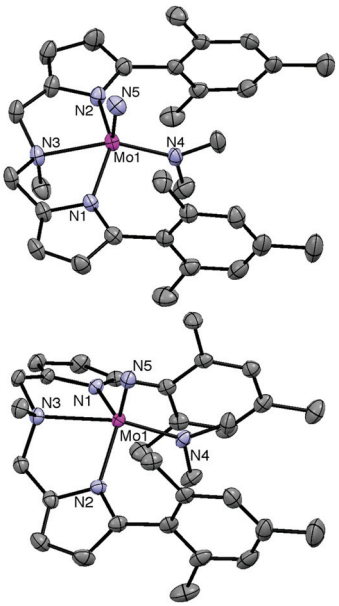

Fig. 3 ORTEP diagram at the 50% probability level for the structures of *anti*-Mo(N)(NMe_2)($dpma^{mes}$) (*anti*-**2**, top) and *syn*-Mo(N)(NMe_2)($dpma^{mes}$) (*syn*-**2**, bottom) as determined by single crystal X-ray diffraction. H-atoms omitted.

isolated in 31% yield. Also found in the reaction mixture were benzyl alcohol (51% yield), benzaldehyde (11% yield), and 1,2-diphenylethane (6% yield), where the yields are relative to internal standard (dodecane) from GC-FID.

The *syn*-isomer also was structurally characterized (Fig. 3 bottom). The structure of *syn*-**2** is, like the structure of **1**, in between sp and tbp with τ = 0.61. The Mo–N(pyrrolyl) and Mo–NMe_2 distances in *syn*-**2** are the same within error as in **1**. The Mo1–N3(donor) and Mo1–N5(nitrido) distances are the same as in *anti*-**2**.

A computational study was carried out on the two isomers using Density Functional Theory with the LANL2DZ basis set as implemented in Gaussian09.[21] The difference in energy ($\Delta H°$) between the *syn* and *anti* derivatives was calculated to be extremely small, with *syn*-**2** being more stable than *anti* by 2 kcal mol^{-1} using B3LYP as the functional. Using B3PW91 as the functional a similar value of 2 kcal mol^{-1} was obtained with *syn* more stable than *anti*. Experimentally, heating *syn*-**2** in toluene at 100 °C for 24 h led to some conversion to the *anti*-**2** isomer (see the ESI† for more details); however, the conversion did not continue to completion and some decomposition also occurred. Only about 9% *anti* was produced during the heating of the *syn* isomer. Alternatively, heating *anti*-**2** did not result in detectable (^{1}H NMR) amounts of *syn*-**2**; only decomposition was observed. It seems that the energies of the isomers are very comparable but kinetic barriers hamper the equilibrium. The isomer, *syn* or *anti*, produced in the reaction of **1** and hydrazine or hydroxylamine is determined kinetically.

Since the hydrazido(1–) derivatives are unstable intermediates in the case of Mo(IV), in order to examine their structure, we prepared the Zr(IV) analogues where no bond cleavage can occur. The zirconium bis(dimethylamido) complex $Zr(NMe_2)_2$-($dpma^{mes}$) (**3**) is cleanly produced by addition of H_2dpma^{mes} to $Zr(NMe_2)_4$; **3** was also structurally characterized (see the ESI†). The addition of one equivalent of H_2NNMe_2 to **3** provides mixtures of the bis(hydrazido(1–)) complex $Zr(NHNMe_2)_2$-($dpma^{mes}$) (**4**) and a trace of a compound not fully characterized that has a ^{1}H NMR spectrum as expected for the mono-(hydrazido(1–)) complex. It appears that the second addition of hydrazine may have a similar rate constant to the first. The complex **4** was prepared cleanly by addition of 2 equivalents of the hydrazine (Fig. 4).

Mechanistic investigations

The reaction between molybdenum-containing **1** and hydrazines was not amenable to typical pseudo-1st order conditions for the examination of the reaction kinetics. Using either the metal complex or the hydrazine in large excess led to very low yields of the nitrido product, and we were unable to isolate and characterize the products under these conditions. However, nitrido product **2** does not react with excess hydrazine on the timescale of the hydrazine reactions with **1**.

Excess hydrazine or **1** in the N–N cleavage reactions leads to unidentified by-product formation; however, we were able to vary the hydrazine concentrations and examine initial rates for the loss of **1**. These experiments suggest a 1st order

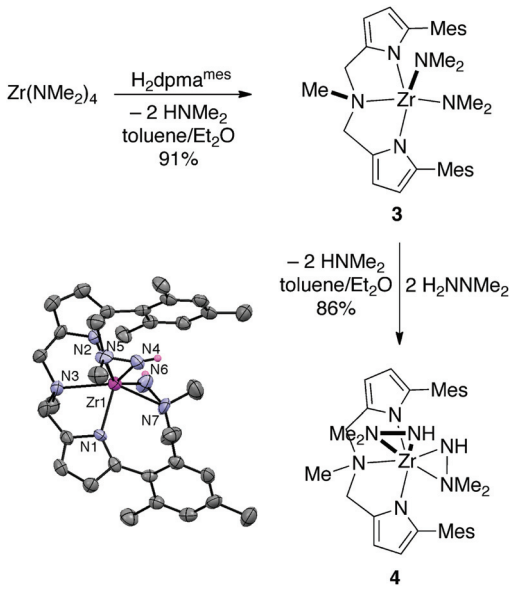

Fig. 4 Synthetic route to the hydrazido(1–) zirconium complex **4** and ORTEP diagram at the 50% probability level for the structure of $Zr(\eta^2\text{-}NHNMe_2)_2(dpma^{mes})$ (**4**) as determined by single crystal X-ray diffraction. H-atoms (pink spheres) are omitted except on the hydrazido(1–) nitrogens N4 and N6.

dependence on hydrazine concentration. Similar initial rate experiments changing metal concentration suggest a 1st order dependence on the concentration of **1**.

Kinetics using 1 : 1 hydrazine to **1** provided clean 2nd order behaviour. Considering the 1st order dependence of the reaction on hydrazine, 1st order dependence on **1**, and 2nd order dependence overall, the rate law is assigned as $-d[\mathbf{1}]/dt = k_{obs}[\mathbf{1}][\text{dimethylhydrazine}]$.

The reaction to form **2** was carried out with a variety of different substrates (Table 1). With all the hydrazine derivatives investigated, *anti*-**2** was the product. There was a dramatic affect of hydrazine substituents on the rate of nitrido formation; however, the cause of that dependence seems complex and is likely due to a mixture of factors including steric constraints of the incoming reactant. Reactions with all of the hydrazines were followed by UV-Vis absorption spectroscopy and fit 2nd order kinetics.

Using the G3 method[22] implemented in Gaussian09, we calculated the Bond Dissociation Enthalpies (BDEs) associated with some of the substrates in Table 1. The BDE of Me_2NNH_2 for the N–N bond was calculated as 60.2 kcal mol^{-1}, whereas the experimental BDE for this compound is 59.0 ± 2.[23] The N–N and N–O BDEs for *N*-aminopyrrole and H_2NOMe (as a model for H_2NOCH_2Ph) were calculated as 34.9 and 54.4 kcal mol^{-1}, respectively. As a result, it appears that the rate of bond cleavage is not correlated with the N–N or N–O BDE.

The only species observed by UV-Vis absorption spectroscopy for all of the hydrazine substrates, except *N*-aminopiperidine, over the course of the reactions are the starting material **1** and the product **2**. These reactions show a clean isosbestic point (see the ESI†). However, the reaction with *N*-aminopiperidine is complicated by reactions of the piperidine by-product with starting material, which is likely the cause of the low yields for this particular substrate. All other amine by-products do not react on the timescales of nitrido formation with either the starting material or product.

No product inhibition was found for the hydrazine reactions except for addition of piperidine to reactions of *N*-aminopiperidine with **1**. Other by-products were tested with up to 10 equivalents of the corresponding amine and gave the same rate constant for disappearance of **1** and provided clean formation of **2**.

The reaction with *O*-benzylhydroxylamine liberates benzyl alcohol as the major by-product. The nitrido product **2** does not react with benzyl alcohol. The starting material **1** does react rapidly with benzyl alcohol using a radical pathway.[24]

We examined the temperature behaviour of the rate of 1,1-dimethylhydrazine reactions with **1**. An Eyring plot of $\ln(k_{obs}/T)$ *vs.* $1/T$ was linear and provided $\Delta H^{\ddagger}$ = +7 kcal mol^{-1} and $\Delta S^{\ddagger}$ = −35 cal mol^{-1} K. These parameters are consistent with a very modest enthalpic barrier and a very ordered activated complex. The parameters are similar to many known activation parameters for ligand additions to metal complexes.[25]

The data above did not conclusively identify the rate-determining step in the reaction. In order to further investigate the NMe_2 for $NHNMe_2$ exchange as a possible rate-determining step, we used the zirconium complex **3** and its reaction with H_2NNMe_2 as a model. The reaction between **3** and two equivalents of dimethylhydrazine was followed by ^1H NMR and showed 2nd-order kinetics like its molybdenum analogue. Examination of the 2nd order rate constant versus temperature for the zirconium reaction gave activation parameters, $\Delta H^{\ddagger}$ = +6.4 kcal mol^{-1} and $\Delta S^{\ddagger}$ = −45 cal mol^{-1} K, similar to the molybdenum system.

We propose that the rate-determining step in the hydrazine reaction with **1** is the dimethylamido substitution step. In zirconium-containing **3**, the second replacement of NMe_2 has a similar rate as the first replacement with dimethylhydrazine (*vide supra*). A second NMe_2 replacement is not observed in the reaction with the molybdenum(IV) analogue. Since the N–N bond cleavage in the reaction of **1** with dimethylhydrazine would then be faster than the substitution of dimethylamido, reaction of the first equivalent of dimethylhydrazine with **1** gives the mono(dimethylamido) complex **2**. The nitrido **2** is then inert to NMe_2 replacement by dimethylhydrazine. In other words, the unimolecular N–N bond cleavage occurs much faster than the bimolecular reaction of hydrazine and the unobserved hydrazido(1–) intermediate $Mo(NHNMe_2)(NMe_2)(dpma^{mes})$.

In light of the data above, we propose the N–N cleavage mechanism illustrated in Scheme 3. One of the dimethylamido ligands in **1** is protolytically replaced with a hydrazido(1–) ligand. We speculate that the unobserved hydrazine adduct **A** adopts a geometry reminiscent of previously reported[18] $Mo(NMe_2)_2(NHMe_2)(dpma)$ where the donor nitrogen of $NHMe_2$ is *trans* to the donor nitrogen of the dpma ancillary.

It appears that it is this bimolecular coordination of the hydrazine (or hydroxylamine) derivative to the metal that is

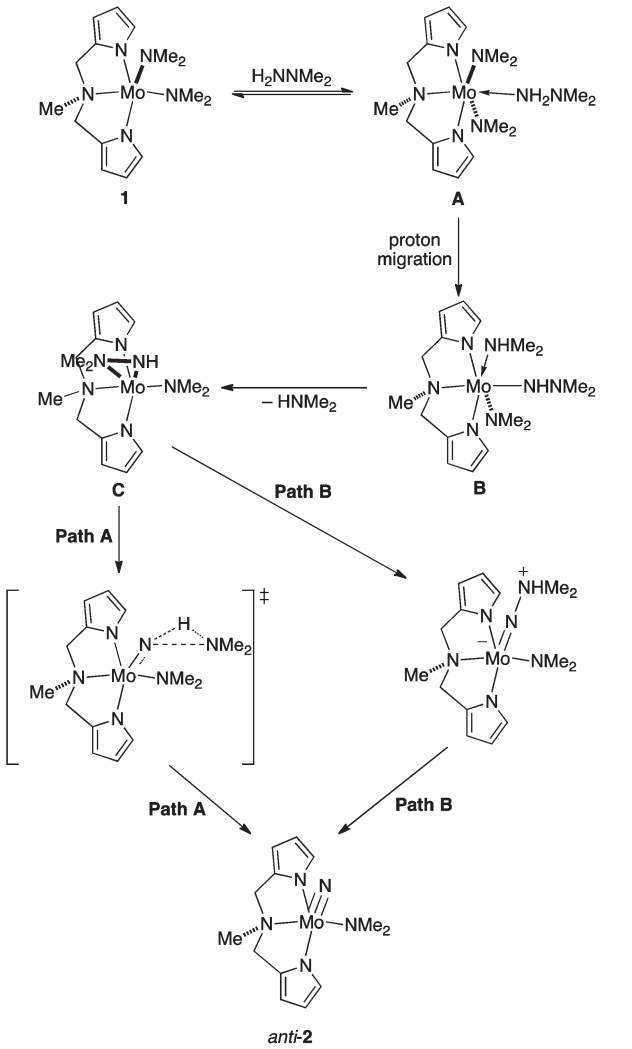

Scheme 3 Proposed mechanism for the reaction of **1** with H_2NNMe_2. Mesityl groups on the $dpma^{mes}$ ligand were omitted for clarity.

rate determining. The alternative rate determining steps are proton migration (conversion from **A** to **B**) or the coordination and proton migration occurring in a concerted fashion. We assign the RDS as the coordination based on the similarity of the activation parameters to other associative substitutions.[24]

In examining various donor ligands with **1**, flat and cylindrically symmetric donors ($CNBu^t$, pyridine, DMAP, and 2-picoline) react extremely quickly with reactions being done faster than samples can be taken. Larger donors such as the hydrazone formed from benzaldehyde and 1,1-dimethylhydrazine, $Me_2NN{=}C(H)Ph$, reacted very slowly over the course of days as judged by disappearance of the UV-Vis bands in **1**. Again, steric constraints of the incoming donor ligand are one factor in the rate of reaction in the system.

After protolytic cleavage of a dimethylamido and dimethylamine loss, formation of the hydrazido(1–) ligand follows. The experiments with the zirconium hydrazido model suggest that the hydrazido(1–) is η^2 in this intermediate.

In the next step, the β-nitrogen of the hydrazido acts as a proton acceptor during the α,β-proton shift. The N–N bond cleavage could occur concomitant with proton migration (Path A) or through an intermediate ammonium hydrazido(2–), sometimes called a hydrazidium (Path B). It is unknown if the actual α,β-proton shift occurs with the aid of another ligand, such as the dimethylamido, or with some other species in solution, such as amine by-product. However, such catalysis in the proton migration is certainly possible considering the computationally derived value for unassisted α,β-proton migration in Mo phosphine systems was assigned a "lower limit" of 17.5 kcal mol^{-1}.[1g]

The reaction mechanism proposed here is an oxidative elimination from a metal-appended nitrogen atom, where the metal is oxidized by elimination of substituents to form a metal ligand multiple bond.[26] Tuczek and coworkers have proposed a similar mechanism in their studies on the Chatt cycle, where the N–N bond cleavage occurs with an α,β-proton shift for molybdenum phosphine complexes.[1g]

In a process that might involve the microscopic reverse of the hydrazine cleavage reaction described, the nucleophilic addition of an amine to a nitrido with concomitant metal reduction has been reported by Meyer and coworkers.[27] In eqn (3) is shown one example, where tpm = tris(1-pyrazolyl)-methane.[28] Several related reductive additions, where the metal center is reduced by addition of substituents to metal ligand multiple bonds have been reported.[29]

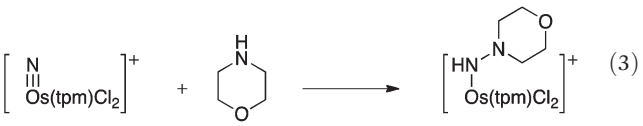

(3)

Whether the nitrido ends up *syn* or *anti* with respect to the methyl on the $dpma^{mes}$ donor nitrogen may be determined by which dimethylamido is kinetically preferred for protolytic replacement in intermediate **A** of Scheme 3. Considering the similarity between the two dimethylamidos, we postulate that this is determined by steric interactions between the complex and hydrazine/hydroxylamine substrate leading to the difference in products observed when using hydrazines and *O*-benzylhydroxylamine. Alternatively, the sites of initial coordination for the larger H_2NNR_2 compounds could be as shown in **A**, while the smaller H_2NOBn may bind in a site similar to the isonitrile in $\mathbf{1}{\cdot}CNBu^t$, *trans* to a dimethylamido (eqn (2)).

Conclusions

We have described a new 5-coordinate Mo(IV) complex with spin crossover behaviour in solution. The free energy barrier for the spin state change was measured as 1150 cm^{-1}. The singlet is the ground state in solution and was the only species observed in the solid, suggesting that molecular dynamics unavailable in the lattice are required for the spin equilibrium.

The Mo(IV) compound reacts with hydrazines and *O*-alkyl hydroxylamines to give the Mo(VI) nitrido complex, NMo(NMe$_2$)(dpma^{mes}) (**2**). Depending on the nature of the nitrogen atom donor molecule (hydrazines or *O*-benzylhydroxylamine), two different isomers of **2** were isolated, one isomer where the methyl group of the dpma^{mes} ligand is *syn* to the nitrido and one where the methyl is *anti*.

We propose a mechanism where the hydrazido(1–) complex undergoes an α,β-proton shift either concerted with N–N bond cleavage or in a stepwise fashion with an unstable hydrazidium, ammonium hydrazido(2–), intermediate.

While the N–N cleavage mechanism proposed in Scheme 3 does not fall into either of the commonly discussed pathways in Scheme 1, there is precedent for this type of mechanism out of the peroxidase literature for O–O bond cleavage (Scheme 4).[30] It is proposed that peroxidase uses an α,β-proton shift in a heme iron peroxide to generate a histidine-stabilized hydrogen isoperoxide complex. Cleavage of the O–O bond, which computationally occurs simultaneously with proton migration (*cf.* Path A in Scheme 3), liberates water and generates the ferryl iron(IV) with a porphyrin radical cation (Compound I).[31]

We propose a very close nitrogen analogue of the peroxidase mechanism is the low energy pathway that leads to facile N–N bond cleavage in our system. Considering, the Tuczek and coworkers proposed similar steps for the Chatt cycle and that the microscopic reverse has also been observed in mid- to late transition metals, this is an important possible pathway for N_2 activation in biological and industrial systems.

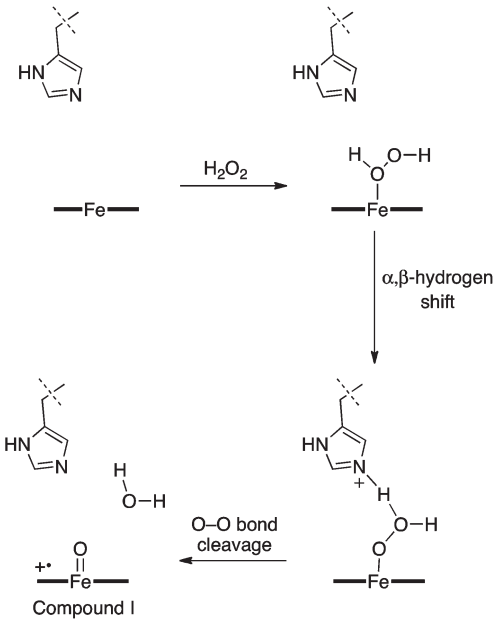

Scheme 4 Poulos–Kraut mechanism[30] for heterolytic O–O cleavage and ferryl generation in peroxidase.

Experimental

General experimental details, tables for the X-ray diffraction experiments, a more thorough discussion on how the kinetic data were collected and the results can be found in the ESI.† NMR data were collected in the Max T. Rogers NMR facility. X-ray diffraction data were collected at the Center for Crystallographic research at MSU.

H_2dpma^{mes}

In a 125 mL Erlenmeyer flask methylamine hydrochloride (0.911 g, 13.5 mmol, 1 equiv.) was dissolved in formaldehyde solution (37% v/v) (2.19 g, 27.0 mmol, 2 equiv.) and EtOH (20 mL). The solution was transferred to a 100 mL Schlenk tube, sealed, and stirred for 10 min in a 55 °C oil bath. 2-Mesitylpyrrole (5.00 g, 27.0 mmol, 2 equiv.) in EtOH (30 mL) was added to the Schlenk tube, and the headspace was evacuated. The solution continued to stir at 55 °C for 7 h, during which a white precipitate formed. The Schlenk tube was cooled to room temperature, and the precipitate was collected on a glass frit and washed with EtOH (3 × 20 mL). The solids were basified with aq. NaOH (1 M, 150 mL) and extracted with CH_2Cl_2 (3 × 100 mL). The organic layers were combined and dried under reduced pressure, yielding H_2dpma^{mes} as a white powder (3.97 g, 9.32 mmol, 69%). ^{1}H NMR (500 MHz, $CDCl_3$): 8.01 (s br, 2H, N–*H*), 6.89 (s, 4H, aromatic C–*H*), 6.07–6.05 (m, 2H, pyrrole C–*H*), 5.92–5.90 (m, 2H, pyrrole C–*H*), 3.53 (s, 4H, CH_2), 2.28 (s, 6H Ar-*p*-CH_3), 2.18 (s, 3H, NCH_3), 2.11 (s, 12H, Ar-*o*-CH_3). ^{13}C{^{1}H} NMR (125 MHz, $CDCl_3$): 138.3, 137.4, 130.9, 129.1, 128.0, 127.9, 108.0, 107.7, 53.5, 41.9, 21.0, 20.6. Anal. Calcd for $C_{29}H_{35}N_3$: C, 81.84; H, 8.29; N, 9.87. Found: C, 81.53; H, 8.32; N, 9.67. Mp: 82–84 °C.

Mo(NMe$_2$)$_2$(dpma^{mes}) (1)

In a glove box under an N_2 atmosphere, a 100 mL Schlenk tube was loaded with a stir bar and a solution of Mo(NMe$_2$)$_4$ [11] (1.00 g, 36.7 mmol, 1 equiv.) in toluene–hexane (1 : 4, 5 : 20 mL). To the Schlenk tube, H_2dpma^{mes} (1.56 g, 3.67 mmol, 1 equiv.) in toluene (8 mL) was added. The headspace was evacuated, and the vessel was sealed with a Teflon stopcock. The tube was removed from the box and was placed into a 55 °C oil bath for 10 h, while stirring vigorously. After this time, the vessel was allowed to cool to room temperature and was taken back inside the dry box. The volatiles were removed *in vacuo*, and the solids were washed with hexane (10 mL). The solids were dissolved in a minimal amount of toluene and held at −35 °C yielding **1** as bright green crystals (1.78 g, 2.94 mmol, 80%). Magnetic susceptibility (Evan's method, 29.7 °C): μ_{eff} = 1.178 μ_B. TOF-MS ES+ calcd (found): 608.68 (609.2). UV-Vis [toluene, 25 °C] λ_{max} in nm (ε in cm^{-1} M^{-1}): 643.9 (498.7), 786.9 (187.4). Mp: 138–144 °C (d). The molecule contains a disordered toluene in the lattice as crystallized. Attempts to obtain elemental analysis were not satisfactory unless toluene was included with occupancy of 0.3. Anal. Calcd for $C_{34}H_{45}MoN_5 \cdot 0.3C_7H_8$: C, 66.36; H, 7.52; N, 11.02. Found: C, 66.60; H, 7.26; N, 11.39.

$Mo(NMe_2)_2(CNBu^t)(dpma^{mes})$ ($1{\cdot}CNBu^t$)

Under an N_2 atmosphere, a scintillation vial was loaded with a stir bar, **1** (0.1 g, 0.165 mmol, 1 equiv.) and toluene (5 mL). To this, *tert*-butylisonitrile (0.1 g, 0.165 mmol, 1 equiv.) in toluene (1 mL) was added. The solution was stirred and rapidly turned dark red. After 1 h, the volatiles were removed *in vacuo*. The residue was extracted with toluene (2 mL). The solution was filtered through Celite and layered with an equal volume of pentane. Crystallization at −35 °C gave dark red crystals of $1{\cdot}CNBu^t$ in 40% yield (0.045 g, 0.066 mmol). Magnetic susceptibility (Evan's method, 28.2 °C): μ_{eff} = 2.469 μ_B. The molecule contains a toluene in the lattice as crystallized. Attempts to obtain elemental analysis were not satisfactory unless toluene was included with full occupancy. Anal. Calcd for $C_{38}H_{54}MoN_6{\cdot}C_7H_8$: C, 69.03; H, 7.98; N, 10.73. Found: C, 68.89; H, 8.17; N, 10.61. Mp: 128–130 °C (dec). UV-Vis [toluene, 25 °C] λ_{max} in nm (ε in cm^{-1} M^{-1}): 372.2 (6588), 490 (3042). Crystals for X-ray diffraction grown from toluene gave poor structural results, and the crystals were regrown from Et_2O.

$Mo(N)(NMe_2)(dpma^{mes})$ (*anti*-**2**)

Under an N_2 atmosphere, a scintillation vial was loaded with a stir bar, **1** (0.650 g, 1.07 mmol, 1 equiv.) and toluene (8 mL). To the stirring solution of **1**, a solution of *N*,*N*-dimethylhydrazine (0.64 g, 1.07 mmol, 1 equiv) in toluene (1 mL) was added. Upon addition, the solution turned brown and an orange precipitate formed. After 1 h, the volatiles were removed *in vacuo*. The residue was stirred in pentane (2 mL) for 5 min, and the suspension was filtered on a glass frit. The solids were collected and dried *in vacuo* yielding the title compound as an orange powder (0.459 g, 0.795 mmol, 75%). Diffraction quality crystals were grown from a concentrated toluene solution layered in pentane held at −35 °C. ^{1}H NMR (500 MHz, C_7D_8): 6.70 (s, 2H, aromatic C–*H*), 6.58 (s, 2H, aromatic C–*H*), 6.37 (d, J_{HH} = 3.0 Hz, 2H, pyrrole C–*H*), 6.17 (dd, J_{HH} = 0.5 Hz, J_{HH} = 3.0 Hz, 2H, pyrrole C–*H*), 4.53 (d, J_{HH} = 13.0 Hz, 2H, CH_2), 3.52 (s, 3H, NCH_3), 3.34 (d, J_{HH} = 12.5 Hz, 2H, CH_2), 2.43 (s, 6H, Ar-*p*-CH_3), 2.18 (s, 3H N(CH_3)$_2$), 2.12 (s, 3H N(CH_3)$_2$), 2.05 (s, 6H, Ar-*o*-CH_3), 2.04 (s, 6H, Ar-*o*-CH_3). ^{13}C{^{1}H} NMR (125 MHz, C_6D_6): 140.8, 140.2, 139.2, 138.4, 136.8, 136.6, 111.2, 106.8, 63.4, 46.5, 43.6, 21.2, 21.0, 20.9. Anal. Calcd for $C_{31}H_{39}MoN_5$: C, 64.46; H, 6.81; N, 12.12. Found: C 64.35; H, 6.72; N, 12.08. Mp: 264–270 °C (dec).

$Mo(N)(NMe_2)(dpma^{mes})$ (*syn*-**2**)

Under an N_2 atmosphere, a scintillation vial was loaded with a stir bar, **1** (0.123 g, 0.202 mmol, 1 equiv.), and toluene (8 mL). To the stirring solution of **1**, a solution of *O*-(benzyl)hydroxylamine (0.750 mL, 0.269 M, 0.202 mmol, 1 equiv.) in toluene (1 mL) was added. Upon addition, the solution turned brown. After 2 h, the volatiles were removed *in vacuo*. The residue was taken up in Et_2O (5 mL) and filtered through Celite. The solution was concentrated *in vacuo* to 2 mL and held at −35 °C, which crystallized **2**-*syn* as orange blocks (0.0356 g, 0.062 mmol, 30.7%). ^{1}H NMR (500 MHz, C_6D_8): 6.79 (s, 2H, aromatic C–*H*), 6.63 (s, 2H, aromatic C–*H*), 6.32 (d, J_{HH} = 3.0 Hz, 2H, pyrrole C–*H*), 6.26 (d, J_{HH} = 3.0 Hz, 2H, pyrrole C–*H*), 3.66 (dd, J_{HH} = 0.5 Hz, J_{HH} = 14.0 Hz, 2H, CH_2), 3.50 (dd, J_{HH} = 0.5 Hz, J_{HH} = 14.0 Hz, 2H, CH_2), 3.20 (d, J_{HH} = 1.0 Hz, 3H, N(CH_3)$_2$), 2.74 (s, 3H, NCH_3), 2.60 (s, 6H, Ar-*p*-CH_3), 2.50 (d, J_{HH} = 1.0 Hz, 3H N(CH_3)$_2$), 2.11 (s, 12H, Ar-*o*-CH_3). ^{13}C{^{1}H} NMR (125 MHz, $CDCl_3$): 139.72, 139.62, 137.23, 136.86, 136.54, 134.77, 128.42, 127.45, 112.15, 106.10, 63.88, 59.31, 53.13, 47.56, 21.35, 20.98, 20.84. Mp: 117–123 °C (dec). By-products of this reaction include benzyl alcohol (51.2%), benzaldehyde (10.7%) and 1,2-diphenylethane (5.9%) as determined by GC-MS/GC-FID; the yields are relative to dodecane internal standard for calibrated samples of those compounds.

$Zr(NMe_2)_2(dpma^{mes})$ (**3**)

Under an N_2 atmosphere, a 100 mL Schlenk tube was loaded with a stir bar, $Zr(NMe_2)_4$ (0.851 g, 3.18 mmol, 1 equiv.), toluene (6 mL), and Et_2O (1 mL). To the pressure tube was added H_2dpma^{mes} (1.35 g, 3.18 mmol, 1 equiv.) in toluene (1 mL). The headspace was evacuated, and the tube was sealed with a Teflon stopcock and removed from the dry box. The solution was stirred in a 70 °C oil bath for 48 h. The tube was taken back into the dry box, and the solution was filtered through Celite. The volatiles were removed *in vacuo* yielding **3** as a yellow powder (1.75 g, 2.89 mmol, 91% yield). ^{1}H NMR (500 MHz, C_6D_6): 6.82–6.81 (m, 2H, aromatic C–*H*), 6.74–6.73 (m, 2H, aromatic C–*H*), 6.30 (dd, J_{HH} = 2.75 Hz, J_{HH} = 0.5 Hz, 2H, pyrrole C–*H*), 6.16 (d, J_{HH} = 3.0 Hz, 2H, pyrrole C–*H*), 4.05 (d, J_{HH} = 13.5 Hz, 2H, CH_2), 3.40 (d, J_{HH} = 13.5 Hz, 2H, CH_2) 2.59 (s, 6H, N(CH_3)$_2$), 2.28 (s, 6H, N(CH_3)$_2$), 2.26 (s, 3H, NCH_3), 2.12 (s, 6H, Ar-*o*-CH_3), 2.10 (s, 6H, Ar-*o*-CH_3), 2.02 (s, 6H, Ar-*p*-CH_3). ^{13}C{^{1}H} NMR (125 MHz, $CDCl_3$): 139.07, 138.61, 138.26, 136.03, 135.94, 135.92, 128.02, 127.47, 127.37, 109.25, 104.71, 59.39, 43.25, 40.63, 39.16, 21.17, 21.01, 20.75. Mp: 262–270 °C.

$Zr(\eta^2\text{-}NHNMe_2)_2(dpma^{mes})$ (**4**)

Under an N_2 atmosphere, a scintillation vial was loaded with **3** (0.100 g, 0.166 mmol, 1 equiv.), a stir bar, and a mixture of toluene and Et_2O (1 : 1 v/v, 8 mL). The solution was rapidly stirred and a 0.712 M toluene solution of 1,1-dimethylhydrazine was added dropwise (466 μL, 0.332 mmol, 2 equiv.). DME (1 mL) was added. The solution stirred for 16 h, and the volatiles were removed *in vacuo*. **4** was obtained in 86% yield as an off-white powder (0.090 g, 1.42 mmol, 86% yield). Diffraction quality crystals of **4** were obtained from a −35 °C concentrated toluene solution layered with Et_2O. ^{1}H NMR (500 MHz, C_7D_8): 6.83 (br s, 2H, aromatic C–*H*), 6.74 (br s, 2H, aromatic C–*H*), 6.25 (d, J_{HH} = 3.0 Hz, 2H, pyrrole C–*H*), 6.14 (dd, J_{HH} = 1.0 Hz, J_{HH} = 3.0 Hz, 2H, pyrrole C–*H*), 4.30 (s, 1H, N*H*), 4.17 (d, J_{HH} = 13.5 Hz, 2H, CH_2), 4.10 (s, 1H, N*H*), 3.68 (d, J_{HH} = 13.5 Hz, 2H, CH_2), 2.48 (s, 3H, NCH_3), 2.30 (s, 6H N(CH_3)$_2$), 2.22 (s, 6H, N(CH_3)$_2$), 2.12 (s, 6H, Ar-*o*-CH_3), 1.91 (s, 3H, Ar-*o*-CH_3), 1.57 (s, 6H, Ar-*p*-CH_3). ^{13}C{^{1}H} NMR (125 MHz, C_6D_6): 140.12, 139.04, 138.91, 138.89, 136.41, 135.63, 128.54, 111.29, 108.21, 104.08, 62.57, 53.49, 50.91, 42.62, 22.44, 21.49, 21.07. Mp: 216–218 °C (dec).

Acknowledgements

The authors would like to thank Kathy Severin and Dan Jones for help in data collection. ALO would like to thank Jim McCusker, Mitch Smith, and Reza Ghiladi for helpful discussions. The financial support of the National Science Foundation CHE-1012537 for this work is greatly appreciated.

Notes and references

1 For some reviews and selected seminal papers see: (*a*) M. D. Fryzuk, *Acc. Chem. Res.*, 2009, **42**, 127; (*b*) P. J. Chirik, *Organometallics*, 2010, **29**, 1500; (*c*) S. Gambarotta and J. Scott, *Angew. Chem., Int. Ed.*, 2004, **43**, 5298; (*d*) N. Hazari, *Chem. Soc. Rev.*, 2010, **39**, 4044; (*e*) Z. Jonas and P. Sobota, *Coord. Chem. Rev.*, 2005, **249**, 2144; (*f*) K. H. Horn, N. Bores, N. Lehnert, K. Mersmann, C. Nather, G. Peters and F. Tuczek, *Inorg. Chem.*, 2005, **44**, 3016; (*g*) A. Dreher, K. Mersmann, C. Nather, I. Ivanovic-Burmazovic, R. van Eldik and F. Tuczek, *Inorg. Chem.*, 2009, **48**, 2078; (*h*) J.-P. F. Cherry, P. L. Diaconescu and C. C. Cummins, *Can. J. Chem.*, 2005, **83**, 302; (*i*) G. Christian, R. Stranger and B. F. Yates, *Chem.–Eur. J.*, 2009, **15**, 646; (*j*) D. V. Yandulov and R. R. Schrock, *Science*, 2003, **301**, 76; (*k*) R. R. Schrock, *Angew. Chem., Int. Ed.*, 2008, **47**, 4415; (*l*) C. E. Laplaza, M. J. A. Johnson, J. C. Peters, A. L. Odom, E. Kim, C. C. Cummins, G. N. George and I. J. Pickering, *J. Am. Chem. Soc.*, 1996, **118**, 8623; (*m*) R. A. Henderson, G. J. Leigh and C. J. Pickett, *Dalton Trans.*, 1989, 425; (*n*) Y. Nishibayashi, *Dalton Trans.*, 2012, **41**, 7447.

2 For some reviews see: (*a*) B. K. Burgess and D. J. Lowe, *Chem. Rev.*, 1996, **96**, 2983; (*b*) Y. Hu and M. W. Ribbe, *Acc. Chem. Res.*, 2010, **43**, 475; (*c*) L. C. Seefeldt, B. M. Hoffman and D. R. Dean, *Ann. Rev. Biochem.*, 2009, **78**, 701.

3 (*a*) G. Ertl, *Angew. Chem., Int. Ed.*, 2008, **47**, 3524; (*b*) R. Schlögl, *Angew. Chem., Int. Ed.*, 2003, **42**, 2004.

4 In FeMo-cofactor of nitrogenase there is also a light element (1st row *p*-block) in the X-ray diffraction experiments. Recent XES studies assert that the central atom in the cluster is a carbon. K. M. Lancaster, M. Roemelt, P. Ettenhuber, Y. Hu, M. W. Ribbie, F. Neese, U. Bergmann and S. DeBeer, *Science*, 2011, **334**, 974.

5 B. M. Hoffman, D. R. Dean and L. C. Seefeldt, *Acc. Chem. Res.*, 2009, **42**, 609.

6 Hydrazido(2–) and isodiazene are two different resonance form participants for M═N–NH_2 ligands. The hydrazido resonance form is considered to be a dianionic ligand, and the isodiazene form is a neutral donor. The situation is very similar to Fischer *versus* Schrock carbenes and depends on the strength of the β-nitrogen lone pair participation. For a discussion see; S. Patel, Y. Li and A. L. Odom, *Inorg. Chem.*, 2007, **46**, 6373.

7 For some examples of diazene pathways see: (*a*) J. L. Crossland, C. G. Balesdent and D. R. Tyler, *Inorg. Chem.*, 2012, **51**, 439; (*b*) C. T. Saouma, C. E. Moore, A. L. Rheingold and J. C. Peters, *Inorg. Chem.*, 2011, **50**, 11285; (*c*) L. D. Field, H. L. Li and A. M. Magill, *Inorg. Chem.*, 2009, **48**, 5.

8 For some representative examples of Mo and W diazenes see: (*a*) M. R. Smith III, T.-Y. Cheng and G. L. Hillhouse, *Inorg.Chem.*, 1992, **31**, 1535; (*b*) M. R. Smith III, T.-Y. Cheng and G. L. Hillhouse, *J. Am. Chem. Soc.*, 1993, **115**, 8638 For a few selected recent examples of diazene complexed with other metals see: (*c*) L. D. Field, H. L. Li and S. J. Dalgarno, *Inorg. Chem.*, 2010, **49**, 6214; (*d*) C. T. Saouma, P. Muller and J. C. Peters, *J. Am. Chem. Soc.*, 2009, **131**, 10358; (*e*) L. D. Field, H. L. Li, S. J. Dalgarno and P. Turner, *Chem. Commun.*, 2008, 1680.

9 (*a*) J. T. Ciszewski, J. F. Harrison and A. L. Odom, *Inorg. Chem.*, 2004, **43**, 3605; (*b*) Y. Li, Y. Shi and A. L. Odom, *J. Am. Chem. Soc.*, 2004, **126**, 1794; (*c*) Y. Li, A. Turnas, J. T. Ciszewski and A. L. Odom, *Inorg. Chem.*, 2002, **41**, 6298; (*d*) C. Cao, J. T. Ciszewski and A. L. Odom, *Organometallics*, 2001, **20**, 5011; (*e*) S. A. Harris, J. T. Ciszewski and A. L. Odom, *Inorg. Chem.*, 2001, **40**, 1987.

10 R. D. Rieth, N. P. Mankad, E. Calimano and J. P. Sadighi, *Org. Lett.*, 2004, **6**, 3981.

11 M. H. Chisholm, F. A. Cotton and M. W. Extine, *Inorg. Chem.*, 1978, **17**, 1329–1332.

12 S. Alvarez and M. Llunell, *Dalton Trans.*, 2000, 3288–3303.

13 S. A. DiFranco, N. A. Maciulis, R. J. Staples, R. J. Batrice and A. L. Odom, *Inorg. Chem.*, 2012, **51**, 1187–1200.

14 (*a*) D. F. Evans, *J. Chem. Soc.*, 1959, 2003; (*b*) D. H. Grant, *J. Chem. Ed.*, 1995, **72**, 39.

15 P. Gütlich, B. R. McGarvey and W. Kläui, *Inorg. Chem.*, 1980, **19**, 3704 Here we replace their $(\Delta\nu/\Delta_0)_{LS}$ with δ' simply because the term was fit as a single parameter. The value of δ' was found to be small, ~0.04 ppm.

16 C. E. Krilley, P. E. Fanwick and I. P. Rothwell, *J. Am. Chem. Soc.*, 1994, **116**, 5225.

17 N. C. Mösch-Zanetti, R. R. Schrock, W. M. Davis, K. Wanniger, S. W. Seidel and M. B. O'Donoghue, *J. Am. Chem. Soc.*, 1997, **119**, 11037.

18 E. Katayev, Y. Li and A. L. Odom, *Chem. Commun.*, 2002, 838.

19 K. M. Wampler and R. R. Schrock, *Inorg. Chem.*, 2007, **46**, 8463.

20 For an example of hydrazine cleavage in a dinuclear tantalum system see: M. P. Shaver and M. D. Fryzuk, *J. Am. Chem. Soc.*, 2004, **127**, 500.

21 M. J. Frisch, G. W. Trucks, H. B. Schlegel, G. E. Scuseria, M. A. Robb, J. R. Cheeseman, G. Scalmani, V. Barone, B. Mennucci, G. A. Petersson, H. Nakatsuji, M. Caricato, X. Li, H. P. Hratchian, A. F. Izmaylov, J. Bloino, G. Zheng, J. L. Sonnenberg, M. Hada, M. Ehara, K. Toyota, R. Fukuda, J. Hasegawa, M. Ishida, T. Nakajima, Y. Honda, O. Kitao, H. Nakai, T. Vreven, J. A. Montgomery Jr., J. E. Peralta, F. Ogliaro, M. Bearpark, J. J. Heyd, E. Brothers, K. N. Kudin, V. N. Staroverov, R. Kobayashi, J. Normand, K. Raghavachari, A. Rendell, J. C. Burant, S. S. Iyengar,

J. Tomasi, M. Cossi, N. Rega, J. M. Millam, M. Klene, J. E. Knox, J. B. Cross, V. Bakken, C. Adamo, J. Jaramillo, R. Gomperts, R. E. Stratmann, O. Yazyev, A. J. Austin, R. Cammi, C. Pomelli, J. W. Ochterski, R. L. Martin, K. Morokuma, V. G. Zakrzewski, G. A. Voth, P. Salvador, J. J. Dannenberg, S. Dapprich, A. D. Daniels, Ö. Farkas, J. B. Foresman, J. V. Ortiz, J. Cioslowski and D. J. Fox, *GAUSSIAN 09 (Revision C.01)*, Gaussian, Inc., Wallingford, CT, 2009.

22 L. A. Curtiss, K. Raghavachari, P. C. Redfern, V. Rassolov and J. A. Pople, *J. Chem. Phys.*, 1998, **109**, 7221.

23 D. F. McMillen and D. M. Golden, *Ann. Rev. Phys. Chem.*, 1982, **33**, 493.

24 S. A. DiFranco and A. L. Odom, manuscript in preparation.

25 A. E. Merbach, *Pure Appl. Chem.*, 1982, **54**, 1479.

26 Compare with a related reaction where a formal M(II) nitrosyl complex is formally oxidized by addition of highly reducing V(III) through intraligand bond cleavage and formation of nitrido.(*a*) A. L. Odom, C. C. Cummins and J. D. Protasiewicz, *J. Am. Chem. Soc.*, 1995, **117**, 6613; (*b*) A. L. Odom and C. C. Cummins, *Polyhedron*, 1998, **17**, 675; (*c*) A. S. Veige, L. M. Slaughter, E. B. Lobkovsky, P. T. Wolczanski, N. Matsunaga, S. A. Decker and T. R. Cundari, *Inorg. Chem.*, 2003, **42**, 6204. Also see redox neutral hydroamination mechanistic proposals where electrocyclic reactions in the ligands are enabled by zirconium. K. Manna, M. L. Kruse and A. D. Sadow, *ACS Catal.*, 2011, **1**, 1637.

27 (*a*) M. H. V. Huynh, E.-S. El-Samanody, K. D. Demadis, T. J. Meyer and P. S. White, *J. Am. Chem. Soc.*, 1999, **121**, 1403 For closely related additions of hydroxylamines to nitridos see: (*b*) M. H. V. Huynh, T. J. Meyer, M. A. Hiskey and D. L. Jameson, *J. Am. Chem. Soc.*, 2004, **126**, 3608 The reverse of the hydroxylamine cleavage, addition of an alcohol to a nitrido has also been reported. (*c*) M. H. V. Huynh, P. S. White, K. D. John and T. J. Meyer, *Angew. Chem., Int. Ed.*, 2001, **40**, 4049.

28 Example in eqn (3) is from ref. 26*a*. The hydrazido(1–), compound 4b in the paper, was characterized as a mixture with its deprotonated hydrazido(2–) derivative in 54% yield.

29 For some selected examples see: (*a*) D. C. Ware and H. Taube, *Inorg. Chem.*, 1991, **30**, 4605; (*b*) T. J. Crevier and T. M. Mayer, *J. Am. Chem. Soc.*, 1998, **120**, 5595; (*c*) T. J. Crevier, B. K. Bennett, J. D. Soper, J. A. Bowman, A. Dehestani, D. A. Hrovat, S. Lovell, W. Kaminsky and J. M. Mayer, *J. Am. Chem. Soc.*, 2001, **123**, 1059; (*d*) A. G. Maestri, K. S. Cherry, J. J. Toboni and S. N. Brown, *J. Am. Chem. Soc.*, 2001, **123**, 7459; (*e*) S. N. Brown, *J. Am. Chem. Soc.*, 1999, **121**, 9752; (*f*) S. N. Brown, *Inorg. Chem.*, 2000, **39**, 378; (*g*) M. H. V. Huynh, P. S. White and T. J. Meyer, *Inorg. Chem.*, 2000, **39**, 2825; (*h*) M. H. V. Huynh, P. S. White and T. J. Meyer, *J. Am. Chem. Soc.*, 2001, **123**, 9170; (*i*) S. B. Seymore and S. N. Brown, *Inorg. Chem.*, 2002, **41**, 462.

30 (*a*) J. D'Antonio and R. A. Ghiladi, *Biochemistry*, 2011, **50**, 5999–6011; (*b*) Y. Ichikawa, H. Nakajima and Y. Watanabe, *ChemBioChem*, 2006, **7**, 1582–1589; (*c*) I. G. Denisov, T. M. Makris and S. Sligar, *J. Biol. Chem.*, 2002, **277**, 42706–42710; (*d*) T. Matsui, S. Ozaki, E. Liong, G. N. Phillips Jr. and Y. Watanabe, *J. Biol. Chem.*, 1999, **274**, 2838–2844; (*e*) H. B. Dunford, W. D. Hewson and H. Steiner, *Can. J. Chem.*, 1978, **56**, 2844–2852; (*f*) M. Kato, S. Aibara, Y. Morita, H. Nakatani and K. Hiromi, *J. Biochem.*, 1984, **95**, 861; (*g*) L. Gebicka and J. Pawlak, *J. Mol. Catal. B: Enzym.*, 1997, **2**, 185.

31 (*a*) T. L. Poulos and J. Kraut, *J. Biol. Chem.*, 1980, **255**, 8199; (*b*) E. Derat and S. Shaik, *J. Phys. Chem. B*, 2006, **110**, 10526.